ACS APPLIED MATERIALS & INTERFACES

Article

Patterning of nanodiamond tracks and nanocrystalline diamond films using a micropipette for additive direct-write processing

Alice Claire Taylor, Robert Edgington, and Richard B. Jackman

ACS Appl. Mater. Interfaces, **Just Accepted Manuscript** • DOI: 10.1021/am507900a • Publication Date (Web): 11 Feb 2015

ACS Publications
High quality. High impact.

ACS Applied Materials & Interfaces is published by the American Chemical Society.
1155 Sixteenth Street N.W., Washington, DC 20036

Patterning of nanodiamond tracks and nanocrystalline diamond films using a micropipette for additive direct-write processing

Alice Taylor, Robert Edgington, Richard B. Jackman*

London Centre for Nanotechnology and Department of Electronic & Electrical Engineering, University College London, 17-19 Gordon Street, WC1H 0AH, UK

Abstract

The ability to pattern the seeding of nanodiamonds (NDs), and thus selectively control areas of diamond growth, is a useful capability for many applications, including photonics, microelectromechanical systems (MEMS) prototyping and biomaterial design. A microprinting technique using a computer–driven micropipette has been developed to deposit patterns of ND monolayers from an unreactive water/glycerol ND ink to a 5μm resolution. The concentration and composition of the ND solutions have been optimised to realise high-density monolayers of NDs and consistent ND printing. Subsequent NCD patterns grown using chemical vapour deposition show a high level of compliance with the printed ND pattern. This ‘direct-write’, bottom-up and additive process offers a versatile and simple alternative to pattern diamond. The process has the particular advantage that it does not require lithography; destructive processing such as reactive ion etching (RIE); and, pertinently, does not involve reactive chemicals that could alter the surface chemistry of NDs. Furthermore, given this process obviates conventional lithography from the process, substrates not suitable for lithographic processing (e.g. excessively small or 3D structured substrates)

can be inscribed with ND patterns. The technique also allows for the growth of discrete, localised, single crystal nanodiamonds with applications in quantum technology.

* Author to whom correspondence should be addressed, r.jackman@ucl.ac.uk

Keywords

Diamond; Nanodiamond; Patterning; Direct-write; Microwave plasma enhanced CVD.

Introduction

The exceptional properties of diamond make it a desirable material for the fabrication of Micro-Electro-Mechanical (MEMS) devices[1,2] due to the attractive tribological[3] and mechanical properties of diamond, as well as high Q-factors being recorded on diamond micro resonators[4]. However, the chemical[5] and electrochemical inertness[6] , and the extreme mechanical stability[7] of diamond make it a difficult material to process. Nanocrystalline diamond films (NCD) produced by chemical vapor deposition (CVD) posses the excellent properties of naturally occurring diamond[8,9], whilst offering the prospect for the selective growth of diamond in specific locations, avoiding the need for 3D pattern generation in thin film diamond layers. Patterned diamond at the micron scale would offer desirable properties for many applications: diamond bio-MEMs are highly desirably due to its biocompatibility[10] and diamonds strong resistance to bacterial colonization[11]. Other examples include diamond used for radio frequency resonators,[12] scanning probe microscopy (SPM) probes as an all diamond cantilever,[13] diamond electrodes for sensor applications,[14] for patterning cells[15-17] and for the fabrication of diamond microelectrode arrays (MEAs)[18-20].

Currently there are several methods to pattern NCD films: top–down reactive ion etching (RIE)[18,21-27], laser ablation, [17,28,29] photolithographic etchants[30] and bottom–up selective nanodiamond (ND) particle seeding, all of which have their own merits. RIE is a destructive process in which photolithographic methods are used in conjunction with typically oxygen / argon RF plasmas to remove unwanted areas of NCD film. RIE patterning is advantageous in that it

fits into conventional CMOS processing work flows and can achieve sub–micrometre resolutions, however difficulties are encountered when etching diamond due to the large resilience of diamond causing low etch selectivities for available hard masks, meaning only shallow diamond films can be easily patterned using such an approach. Furthermore, O_2/Ar RF plasmas can be damaging to the underlying substrate materials upon which NCD is deposited. More recently selective seeding has emerged as a solution to counter the low selectivity of diamond RIE processing to allow the bottom-up patterning of ND and NCD films. Various methodologies have been employed to pattern ND seeds, including inkjet printing of diamond inks[31,32], microcontact printing[33] and ND seeding via electrostatic self-assembly.[34]. While these methods avoid the problems associated with mask selectivity in diamond etching, photolithography is still required and residual NDs can remain in nominally void pattern areas, leading to diamond growth in unwanted regions. To avoid this issue, Hérbert *et al.* combine both processes by seeding with NDs, 'fixing' NDs with a short CVD plasma exposure, removing ND seeds from void pattern areas with RIE, and subsequently growing patterned NDs into NCD films[35].

Whilst all of these techniques have their merits, these processes still require photolithographic steps and the application of corrosive or reactive chemicals in processing, which could effect the surface chemistry of deposited NDs. Here a novel direct–write selective seeding method is described where no photolithographic steps or corrosive chemicals are required. ND patterns are

deposited using a micropipette, which can print a variety of solutions onto desired substrates in picolitre volumes via ultrasonic ejection of liquid. 'Ink' constitution and printing parameters have been optimized, and the effect of varying micropipette diameter investigated. Post–printing, water and glycerol from the ink are evaporated at low pressures and temperatures to produce ND coatings of near monolayer thickness in any desired pattern. Subsequent CVD growth leads to patterned NCD layers. This direct–write additive method allows for facile microfabrication of nanodiamond patterns on a variety of substrates and topographies, unlike photolithographic techniques, which are limited to planar surfaces and require corrosive chemicals. Finally, this method has minimal wastage of NDs and can efficiently coat substrates using very small ND amounts, which is very important for applications where sample amounts are scarce, such as the positioning of NDs with colour centres (e.g. nitrogen–vacancy centres) on substrates.

Experimental methods

Selective printing

A GIX II Microplotter (purchased from www.sonoplot.com) was used in ambient conditions for the selective seeding of ND inks. The microplotter is a computer–controlled micropipette fluid dispensing system for the deposition of picolitre volumes of liquid to 5μm precision. Liquids are drawn into the pipette from an ink well via capillary action and ejected via application of ultrasound to the pipette when in meniscal contact with a surface. The ultrasonic

intensity is sufficiently low to avoid a spray ejection of liquid. The software programme SonoDraw was used to design the desired patterns in which the ink would be printed on the surface. An applied piezo-voltage of 20 V was used for every print as this was found produce the most reliable and consistent printing. Printing speeds were varied from 100 μm s^{-1} to 10000 μm s^{-1} depending on the substrate and tip; typically 2000 μm s^{-1} for silicon and 1000 μm s^{-1} for glass. Glass micropipettes were produced using a p-97 flaming/brown horizontal micropipette puller. Pulling parameters were optimised in order to produce a range of tips with inner diameters ranging between 1 μm to 30 μm.

Chemicals

Monodispersed detonation nanodiamonds (DNDs) (6–10 nm) were used throughout (New Metals & Chemicals Corporation, Japan). Various inks containing DNDs and glycerol (99.0% Sigma Aldrich, MW: 92.09 $gmol^{-1}$, 1414 cP) were produced and subjected to ultra-high power sonication using a VCX500 Vibra-cell sonicator with the cup horn accessory (100% amplitude, 3:2 duty cycle, water cooled and temperature controlled to be <28˚C, 5 hrs) to fully disperse the DNDs and to ensure a thorough glycerol / de–ionised water mix.

Substrate cleaning

Substrates were degreased in acetone, IPA and then DI water (each for 5 mins sonication), to remove residues and dirt. Dust free surfaces allow for higher resolution printing, with reduced flow-back and also reduced

contamination of particulates in the clean ND ink. With contamination, the NCD film quality suffers, as these particles act as re–nucleation sites and so the film contains more grain boundaries, and so all substrates are thoroughly cleaned before use.

Ink evaporation

A vacuum chamber (10^{-3} mbar, 50°C, 5mins) was used to evaporate the glycerol / de-ionised water ink and leave the printed NDs in the desired pattern on the surface of the substrate. Vacuum evaporation was used to allow glycerol evaporation at low temperatures as to not oxidise NDs through heating (oxidation onset ~ 250˚C). The boiling point of glycerol at 10^{-3} mbar is 40°C, and so a temperature of 50°C was used to ensure all glycerol had evaporated. In order to obtain a regular seeding of NDs on the surface, it is important that a quick evaporation of the ink is done. This helps to minimise the 'coffee-ring' effect, by where the ink dries towards the edge of the print, leaving a higher concentration of NDs around the ring.

Atomic Force Microscopy

AFM measurements were carried out using a Veeco Dimension V using aluminum coated silicon AFM probes (resonant frequency 190 kHz). The system was operated in tapping mode with a VT-103-3K Acoustic/ Vibration Isolation System and the VT-102 Vibration Isolation Table at room temperature in air. AFM analysis was performed on ND patterns of varying ND concentrations, post–evaporation, with a scan size of 2 μm. AFM Images

were post–processed with a median filter (3x3 kernel) using MATLAB 2012a software to remove noise and measurement artefacts. Surface coverage of NDs as a percentage was calculated using the threshold feature on ImageJ software.

Patterned Nanocrystalline Diamond growth

Nanodiamond micro-patterns were printed on degreased Si (native oxide), SiO_2 (PECVD) and quartz wafers (5 mins acetone, 5 mins isopropanol alcohol, 5 mins deionised water with low power ultrasonication and N_2 gun drying). Print patterns were drawn on Sonodraw 1.1.3 software. Following ink evaporation, Microwave-plasma enhanced CVD (MPECVD) was performed using a SEKI Model AX5010 PECVD reactor. The parameters for growth were: 1500 W, 200 sccm H_2, 1.4 sccm CH_4 (0.7%), with 30 min and 4 hr growth times and a 5 minute 5% CH_4 initial incubation period.

Scanning Electron Microscopy

Both the glass micropipettes and the NCD patterns were characterised using a Carl Zeiss XB1540 focussed-ion-beam microscope with an accelerating voltage of 5kV.

Results and discussion

Optimising ink deposition

In order to achieve consistent and contiguous liquid deposition from a microplotter, optimisation of ink viscosity is essential. Various inks were

prepared containing varying ratios of glycerol and de-ionised (DI) water and dynamic viscosities were calculated using the parameterisation stated by Cheng (2008)[36]. The viscosity of glycerol at 20°C is much greater than water (1414 cP compared to 1.75 cP), the optimum viscosity for printing was found to be a mixture of 50% volume glycerol, 50% de-ionised water (4.83 cP), as illustrated in figure 1(a), with the values for the dynamic velocity of the ink plotted in figure 1(b). This ink had a low enough viscosity to allow effective flows from the tip, high enough to prevent reflow and clumping of the ink at pattern vertices.

In addition to improving print quality, glycerol reduces the evaporation rate of water due to the increase in intermolecular forces, which avoids the premature evaporation of ink and the uneven deposition of NDs biased towards the edges of features where evaporation concludes, i.e. the 'coffee–ring" effect. Whilst glycerol reduces premature evaporation of the ink, the boiling point of glycerol at room pressure is 290 °C, such temperatures could cause substrate damage and there have been reports of ND oxidation occurring at temperatures as low as 300 °C[37], which might lead to surface modification. Hence a custom vacuum chamber was built to enable the use of a lower vapour pressure of glycerol. A pressure of below 10^{-3} mbar was used to allow the evaporation of glycerol at 50˚C, being sufficiently low to avoid chemical modification of the NDs.

ND concentration

Having established an optimum ink viscosity, the effect of changing concentration of the NDs was investigated. In order to grow high quality NCD

patterns it is important that the ND assembly on the surface coverage is as confluent and as close to monolayer as possible, as small particles (rather than aggregates) results in better uniformity of the film[38]. Therefore it was important to ascertain which ND concentration produced confluent ND seeding and near monolayer coverage, as to optimise subsequent NCD film growth and minimise ND usage. The effect of ND concentration on seeding was investigated using AFM.

Figure 2(a) shows AFM images of NDs seeded on silicon using a 30 μm tip and dot printing, with inks printed in concentrations of NDs ranging from 0.025 to 0.15 gL^{-1}, following glycerol-DI water evaporation. The corresponding graph, Figure 2(b), shows the percentage coverage of the surface in relation to the ND concentration. It can be seen that for concentrations of 0.1 gL^{-1} and above, the coverage is 100%. For concentrations less than 0.1 gL^{-1} coverage is incomplete, for example, at 0.75 gL^{-1} coverage was 82%. The monolayer-type coverage observed shows evidence of the occasional small aggregate being present in the printed region, this is better than other reported attempts at printing ND patterns. For example, Zhuang *et al.* used a microcontact printing technique for producing ND patterns and the method was reported to only able to transfer ND agglomerates, and not individual ND particles[33]. As NCD quality is dependent on the size of the seed material and its uniformity, the method described here offers the prospect of better, denser, NCD films.

Patterning

Figure 3 shows SEM images of CVD grown patterned NCD on silicon substrates with the ND seeds printed with a 0.1 gL^{-1} ND 50% wt glycerol / DI

water ink. The ND patterns were grown for 30 minutes – 4 hours (see figure captions for duration) using previously stated conditions. Figure 3(a) shows an array of lines printed using a tip with an inner diameter (ID) of 5μm, the lines are 200 μm spaced and their width is approx. 7μm. Consistent and clean printed lines are observed with a high level of pattern compliance and no residual NDs in void pattern regions. Figure 3(b, c) show lines printed on Si using a 5 μm ID tip. It can be seen that the edge (Figure 3(d)) of the lines are clean and no additional processes are needed for the removal of unwanted NCD. Figure 3(e) The edge of a printed grid showing two intersecting lines, tip size 5 μm ID. Figure 3(f) shows NCD printed with a void square in the middle, sharp lines and corners are observed, highlighting the high resolution of the printing method. Figure 3(g) shows the thinnest line achieved using this printing method, the line width is approximately 2 μm and was printed using a tip with an ID of 1.5 μm. Figure 3(h) shows a 100μm spaced array of printed NCD dots. Figure 3(i) shows one printed dot, with a diameter of approximately 20μm, which was achieved using a tip with an ID of 15μm. Figure 3(j) shows the edge of the printed dot shown in figure 3(i), clean printed edges are observed. The resolution of printing is limited to the mechanical movement of the machine, which has a 5 μm positioning resolution, and also to ID size of the pipette and ultrasonic power of the piezoelectric. Printed line artefacts are due to the slightly uneven motion of the tip during the print, but can be minimised by securing the substrate whilst printing and altering the speed of the print accordingly. SonoDraw 1.1.3 software allows for the patterning of lines, dots, arcs and filled regions, so any desired shape can be printed using this method. Figure 3(k) SEM shows high quality NCD, verified by the faceted

texture of the NCD film, as well as the confluent, pinhole–free nature of the film, all of which can be ascribed to high–density, homogenous seeding. Figure 3(l) was grown from a printed region where the ND concentration in the ink was 0.001 gl^{-1}; this resulted in an individual ND being grown into a small (~500 nm) single crystal diamond. This capability is also of considerable interest since individually-placed fluorescent NDs are key to several quantum information processing applications that are currently under investigation.

Tip diameter vs. dot diameter

In order to investigate the effect of ID on dot deposition, a set of tips with varying diameter were prepared for printing. Different sized tips were pulled using a horizontal micropipette puller, whereby controlling the speed of the tip pull changes the ID. The ID of tips ranged from 1 to 30 μm. Figure 4(a-d) show different tips of graded diameters alongside SEM images of their corresponding NCD dots on Si surfaces. All ND dots were subject to 30 mins growth using normal NCD conditions as previously stated. The minimum size of micropipette that can successfully print is 1.5μm. When attempting to print smaller than this, ink did not enter the micropipette due to capillary action failing to load the pipette. Fig 4e shows the relationship between tip ID and NCD dot diameter (DD). The relationship is approximately linear, where the printed dot is slightly larger than the tip ID ($DD \approx 3.15 + 1.40ID$). For a 30μm tip, the dot is roughly 45μm and so an ink spreading of ca. 40% is observed. Micropipettes with an inner diameter of 30μm were found to produce the most consistent printing.

NCD quality was investigated by SEM and Raman spectroscopy. One of the

most important factors in determining the quality of thin film diamond is surface roughness. The seeding quality and density of the nanodiamonds is paramount to this.[39] Various scratching and seeding techniques have been used to enhance ND nucleation density on foreign substrates. Scratching often results in a high nucleation density because the large diamond particles are imperfect and thus chip along grain boundaries leaving smaller diamond particles on the surface, which act as the nucleation site.[40] In order to obtain ND near–monolayer patterns it is important to sonicate the ink immediately before printing, this ensures that the NDs are fully dispersed in solution, and as few as possible aggregates are present. Best results were achieved when ND inks were sonicated for at least 8 hours immediately before printing. Nicely faceted NCD (4 hour growth) can be see using SEM in figure 3(e), confirming the quality of the ND seeding.

Figure 5 shows the Raman spectra of the grown NCD, the diamond peak is observed at 1333 cm^{-1} for the 30 min growth, and 1329 cm^{-1} for the 4 hour growth. This peak corresponds to the zero–phonon line of diamond, indicative of a high content of sp^3–bonded carbon. Peak broadening can be observed in the sp^3 peak for the 30 min growth due to the low crystallite size of diamond grains and the thinness of the film[41], and the redshift of the peak arises in phonon confinement in the NCD and is linear with grain size[42]. The narrowing of this peak at 4 hours growth suggest that the film grain size is approaching the micro-scale. The broad peak observed at 1560 cm^{-1} in the 30 min growth spectrum shows evidence of the non-diamond G-band, which arises from sp^2 carbon in-plane stretching mode, which can be assumed to be at the grain boundaries.[43]

Conclusion

An additive, lithography–free, inert bottom-up technique for producing nanodiamond tracks and nanocrystalline diamond patterns with a high pattern compliance has been established, with a lateral resolution of 5μm and feature widths of ca. 2 μm. Patterning is achieved without the use of reactive chemicals, allowing for the preservation of ND surface chemistry. The patterning procedure has been developed using ultrasound driven plotter to deposit nanodiamond and glycerol / DI water inks. Printing has been optimised by tailoring ink constitution, hardware parameters and micropipette tip diameter to produce ND patterns with near–monolayer coatings with few agglomerates present. The effect of varying ND concentration upon ND seeding has been studied, and the relationship between tip diameter and dot size identified. Furthermore, low density ND patterning is demonstrated, which makes this process a valuable method for studying the individual properties of NDs on substrates, for example for quantum information processing applications. Post–printing, ink solvents are evaporated off using a low temperature vacuum evaporation to leave NDs in the desired pattern. The resultant ND patterns have been used as the nucleation site for NCD growth, and suspending the NDs in glycerol has no observable effects in the quality of the diamond film. Pertinently, this patterning technique allows for the selective seeding of NDs on a variety of substrates, including 3D substrates not compatible with conventional lithography techniques, and with a high degree of control over the nature of the ND monolayers deposited. This

method for diamond patterning provides a material type that has lots of potential applications, which range from the use as a photonic crystal[44], to the use in bioelectronics[45] and MEMS applications including piezoelectric micro-resonators[46].

Acknowledgements

This work was performed as part of a EU F7 project 'NEUROCARE' (number 280433-2) and was partially supported by the UKs Engineering and Physical Sciences Research Council (EPSRC, EP/F026110/1).

References

(1) Luo, J. K.; Fu, Y. Q.; Le, H. R.; Williams, J. A.; Spearing, S. M.; Milne, W. I. Diamond and Diamond-like Carbon MEMS. *J. Micromech. Microeng.* **2007**, *17*, S147–S163.

(2) Bongrain, A.; Scorsone, E.; Rousseau, L.; Lissorgues, G.; Gesset, C.; Saada, S.; Bergonzo, P. Selective Nucleation in Silicon Moulds for Siamond MEMS Fabrication. *J. Micromech. Microeng.* **2009**, *19*, 074015.

(3) Williams, J. A.; Le, H. R. Tribology and MEMS. *J. Phys. D: Appl. Phys.* **2006**, *39*, R201–R214.

(4) Lu, J; Cao, Z; Aslam, D; Sepúlveda, N; Sullivan, J. Diamond Micro and

Nano Resonators using Laser Capacitive or Piezoresistive Detection. IEEE Int. Conf. Nano/Micro Eng. Mol. Syst., 3rd 2008.

(5) Krueger, A. Beyond the Shine: recent progress in Applications of Nanodiamond. *Lab Chip* **2011**, *21*, 12571.

(6) Fries, M. D.; Vohra, Y. K. Properties of Nanocrystalline Diamond Thin Films grown by MPCVD for Biomedical Implant Purposes. *Diamond Relat. Mater.* **2004**, *13*, 1740–1743.

(7) May, P. W. Diamond Thin Films: a 21st-century Material. Philos. Trans. R. Soc., A **2000**, *358*, 473–495.

(8) Williams, O. A.; Nesladek, M. Growth and Properties of Nanocrystalline Diamond Films. Phys. Status Solidi A. **2006**, 203, 13, 3375–3386.

(9) Philip, J.; Hess, P.; Feygelson, T.; Butler, J. E. Elastic, Mechanical, and Thermal Properties of Nanocrystalline Diamond Films. *J. Appl. Phys.* **2003**, 93, 2164–2171.

(10) Tang, L.; Tsai, C.; Gerberich, W. W.; Kruckeberg, L.; Kania, D. R. Biocompatibility of Chemical-Vapour-Deposited Diamond. J. Neurosci. Methods **1995**, *16*, 483–488.

(11) Jakubowski, W.; Bartosz, G.; Niedzielski, P. Nanocrystalline Diamond Surface is Resistant to Bacterial Colonization. *Diamond Relat. Mater.* **2004**, 13, 1761–1763.

(12) Mortet, V.; Williams, O. A.; Haenen, K. Diamond: a Material for Acoustic Devices. Phys. Status Solidi A. **2008**, *205*, 1009–1020.

(13) Malavé, A.; Oesterschulze, E. All–diamond Cantilever Probes for Scanning Probe Microscopy Applications Realized by a Proximity

Lithography Process. *Rev. Sci. Instrum.* **2006**, *77*, 043708.

(14) Pedrosa, V. A.; Miwa, D.; Machado, S. A. S.; Avaca, L. A. On the Utilization of Boron Doped Diamond Electrode as a Sensor for Parathion and as an Anode for Electrochemical Combustion Of Parathion. *Electroanalysis* **2006**, *18*, 1590–1597.

(15) Regan, E. M.; Taylor, A.; Uney, J. B.; Dick, A. D.; May, P. W.Spatially Controlling Neuronal Adhesion and Inflammatory Reactions on Implantable Diamond, IEEE JETCAS, **2011**, 1, 557–565.

(16) Edgington, R. J.; Thalhammer, A.; Welch, J. O.; Bongrain, A.; Bergonzo, P.; Scorsone, E.; Jackman, R. B.; Schoepfer, R. Patterned Neuronal Networks using Nanodiamonds and the Effect of Varying Nanodiamond Properties on Neuronal Adhesion and Outgrowth. *J. Neural Eng.* **2013**, *10*, 056022.

(17) May, P. W.; Regan, E. M.; Taylor, A.; Uney, J.; Dick, A. D.; Mcgeehan, J. Spatially controlling neuronal adhesion on CVD diamond. *Diamond Relat. Mater.* **2012**, *23*, 1–5.

(18) Bonnauron, M.; Saada, S.; Rousseau, L.; Lissorgues, G.; Mer, C.; Bergonzo, P. High Aspect Ratio Diamond Microelectrode Array for Neuronal Activity Measurements. *Diamond Relat. Mater.* **2008**, *17*, 1399–1404.

(19) Bergonzo, P.; Bongrain, A.; Scorsone, E.; Bendali, A.; Rousseau, L.; Lissorgues, G.; Mailley, P.; Li, Y.; Kauffmann, T.; Goy, F.; Yvert, B.; Sahel, J. A.; Picaud, S. 3D shaped Mechanically Flexible Diamond Microelectrode Arrays for Eye Implant Applications: The MEDINAS project. *IRBM* **2011**, *32*, 91–94.

(20) Cottance, M.; Nazeer, S.; Rousseau, L.; Lissorgues, G.; Bongrain, A.; Kiran, R.; Scorsone, E.; Bergonzo, P.; Bendali, A.; Picaud, S.; Joucla, S.; Yvert, B. *Diamond Micro-electrode Arrays (MEAs): A new route for In–Vitro Applications*. DTIP, **2013**, 1–4.

(21) Taniguchi, J.; Tokano, Y.; Miyamoto, I.; Komuro, M.; Hiroshima, H. Diamond Nanoimprint Lithography. *Nanotechnology* **2002**, *13*, 592–596.

(22) Ding, G.; Yao, J.; Yu, A.; Zhao, X.; Wang, L.; Shen, T. Paterning of Diamond Films by RIE and its MEMS Aplications. In Micromachining and Microfabrication Process Technology VI. In; Karam, J. M.; Yasaitis, J. A., Eds. SPIE, **2000**, 4174, 451–461.

(23) Ramanathan, M.; Darling, S. B.; Sumant, A. V.; Auciello, O. Nanopatterning of Ultrananocrystalline Diamond Thin Films via Block Copolymer Lithography. *J. Vac. Sci. Technol., A* **2010**, *28*, 979–983.

(24) Ando, Y.; Kuwabara, J.; Suzuki, K.; Sawabe, A. Patterned Growth of Heteroepitaxial Diamond. *Diamond Relat. Mater.* **2004**, *13*, 1975–1979.

(25) Maybeck, V.; Edgington, R.; Bongrain, A. Welch, J. O.; Scorsone, E.; Bergonzo, P.; Jackman, R. B.; Offenhäusser, A. Boron-Doped Nanocrystalline Diamond Microelectrode Arrays Monitor Cardiac Action Potentials. Adv. Healthcare Mater. **2014**, 3, 283–289.

(26) Domonkos, M.; Izak, T.; Stolcova, L.; Proska, J.; Kromka, A. Fabrication of Periodically Ordered Diamond Nanostructures by Microsphere Lithography. Phys. Status Solidi B **2014**, *251*, 2587–2592.

(27) Wang, X. D.; Hong, G. D.; Zhang, J.; Lin, B. L.; Gong, H. Q.; Wang, W. Y. Precise Patterning of Diamond Films for MEMS Application. *J. Mater. Process. Technol.* **2002**, *127*, 230–233.

(28) Narayan, J.; Chen, X. Laser Patterning of Diamond Films. *J. Appl. Phys.* **1992**, *71*, 3795.

(29) Ral'Chenko, V. G.; Korotushenko, K. G.; Smolin, A. A. Fine Patterning of Diamond Films by Laser-assisted Chemical Etching in Oxygen. *Diamond Relat. Mater.* **1995**. 4, 893–896.

(30) Shimoni, O.; Cervenka, J.; Karle, T. J.; Fox, K.; Gibson, B. C.; Tomljenovic-Hanic, S.; Greentree, A. D.; Prawer, S. Development of a Templated Approach to Fabricate Diamond Patterns on Various Substrates. *ACS Appl. Mater. Interfaces* **2014**, *6*, 8894–8902.

(31) Chen, Y.-C.; Tzeng, Y.; Cheng, A.-J.; Dean, R.; Park, M.; Wilamowski, B. M. Inkjet Printing of Nanodiamond Suspensions in Ethylene Glycol for CVD Growth of Patterned Diamond Structures and Practical Applications. *Diamond Relat. Mater.* **2009**, *18*, 146–150.

(32) Fox, N. A.; Youh, M. J.; Steeds, J. W.; Wang, W. N. Patterned Diamond Particle Films. *J. Appl. Phys.* **2000**, *87*, 8187–8191.

(33) Zhuang, H.; Song, B.; Staedler, T.; Jiang, X. Microcontact Printing of Monodiamond Nanoparticles: An Effective Route to Patterned Diamond Structure Fabrication. *J. Phys. Chem. C* **2011**, *27*, 11981–11989.

(34) Lee, S.-K.; Kim, J.-H.; Jeong, M.-G.; Song, M.-J.; Lim, D.-S. Direct Deposition of Patterned Nanocrystalline CVD Diamond using an Electrostatic Self-assembly Method with Nanodiamond Particles.

Nanotechnology **2010**, *21*, 505302.

(35) Hebert, C.; Scorsone, E.; Bendali, A.; Kiran, R.; Cottance, M.; Girard, H. A.; Degardin, J.; Dubus, E.; Lissorgues, G.; Rousseau, L.; Picaud, S.; Bergonzo, P. Boron doped Diamond Biotechnology: from Sensors to Neurointerfaces. *Faraday Discuss.* **2014**, 172, 47–59.

(36) Cheng, N.-S. Formula for the Viscosity of a Glycerol−Water Mixture. *Ind. Eng. Chem. Res.* **2008**, *47*, 3285–3288.

(37) Kulakova, I. I. Surface chemistry of nanodiamonds. *Phys. Solid State* **2004**, *46*, 636–643.

(38) Ascarelli, P.; Fontana, S. Dissimilar Grit-size Dependence of the Diamond Nucleation Density on Substrate Surface Pretreatments. Appl. Surf. Sci. **1993**, *64*, 307–311.

(39) Williams, O. A. Nanocrystalline Diamond. *Diamond Relat. Mater.* **2011**, *20*, 621–640.

(40) Avigal, Y.; Hoffman, A. A new method for nucleation enhancement of diamond. *Diamond Relat. Mater.* **1999**. 8, 127–131.

(41) Osswald, S.; Mochalin, V. N.; Havel, M.; Yushin, G.; Gogotsi, Y. Phys. Phonon Confinement Effects in the Raman Spectrum of Nanodiamond. *Phys. Rev. B* **2009**, 80, 075419.

(42) Sun, K. W.; Wang, J. Y.; Ko, T. Y. Raman Spectroscopy of Single Nanodiamond: Phonon-confinement Effects. *Appl. Phys. Lett.* **2008**, *92*, 153115.

(43) Ferrari, A.; Robertson, J. Interpretation of Raman spectra of Disordered and Amorphous Carbon. *Phys. Rev. B* **2000**, *61*, 14095–14107.

(44) Ondič, L.; Dohnalová, K.; Ledinský, M.; Kromka, A.; Babchenko, O.; Rezek, B. Effective Extraction of Photoluminescence from a Diamond Layer with a Photonic Crystal. *ACS Nano* **2011**, *5*, 346–350.

(45) Nebel, C. E.; Shin, D.; Rezek, B.; Tokuda, N.; Uetsuka, H.; Watanabe, H. Diamond and Biology. J. R. Soc., Interface. **2007**, 4, 439–461.

(46) Hees, J.; Heidrich, N.; Pletschen, W.; Sah, R. E.; Wolfer, M.; Williams, O. A.; Lebedev, V.; Nebel, C. E.; Ambacher, O. Piezoelectric Actuated Micro-resonators based on the Growth of Diamond on Aluminum Nitride thin Films. *Nanotechnology* **2012**, *24*, 025601.

Figure captions

Figure 1

(a) Optical microscope images of grids printed using ND containing inks on a glass substrate. The three images are varying in glycerol percentage with it increasing from left to right. Optimum printing is observed using an ink containing 50 % glycerol. (b) The viscosity of the solution is calculated in related to the percentage weight of glycerol. Optimum viscosity was found to be 6.04 cP.

Figure 2

(a) 2 μm square AFM images of NDs seeded on silicon, each image is of NDs after evaporation of a glycerol de-ionised water ink, the resultant NDs are left seeded on the surface in varying coverage dependent on the concentration of NDs in the ink, concentrations shows are 0.025 gl^{-1}, 0.05 gl^{-1}, 0.075 gl^{-1}, 0.1 gl^{-1}. Scans are representative of the whole patterned area and were selected at random over each print. (b) Corresponding percentage coverage of NDs on Si in relation to concentration of NDs in the ink.

Figure 3

SEM images of patterned NCD which have been grown on silicon substrates using printed NDs as the seed and MWPECVD for the growth, all inks consisting of 50% wt glycerol and NDs at a concentration of 0.1 gl^{-1}, growth times varied from 30 minutes – 4 hours, 1500 W, 50 torr and 0.7 % CH_4. (a–c) A series of lines printed using a 5 μm ID tip, line width approx. 7 μm. Growth

for 30 minutes. (d) The egde of the printed line shown in (c). (e) The edge of a printed grid showing two intersecting lines, tip size 5 μm ID, growth for 30 minutes. (f) NCD outline of square grown for 4 hours. (g) Line printed using 1.5 μm ID pipette, line width ≈ 2 μm. Grown for 30 minutes. (h) An array of dots printed using a 15 μm ID tip, grown for 1 hour. (i) An individual printed NCD dot from (h). (j) Edge of printed dot shown in (i). (k) Zoomed in SEM of the surface of a printed NCD region after 30 minute growth. (l) An ND seed grown into an individual NCD grain grown for 4 hours.

Figure 4

(a-d) SEM images of horizontally pulled glass micro-pipettes (left hand column) and the corresponding printed ND dot which has been grown into NCD (right hand column). Velocity of the pull was altered to produce micro-pipettes with the desired inner diameter. The velocity is in an arbitrary unit, but range from (a) 8 a.u. to (d) 14 a.u, producing tips with an inner diameter of around 40 μm to 5 μm respectively. (A tip with an ID of 1.5 μm has been pulled but SEM is not available). (e) Corresponding graph showing how the micropipette inner diameter affects the diameter of the NCD dot.

Figure 5

Raman spectra of NCD dots grown for 30 mins and 4 hours, both spectra showing the zero-phonon line for present in diamond thin films.

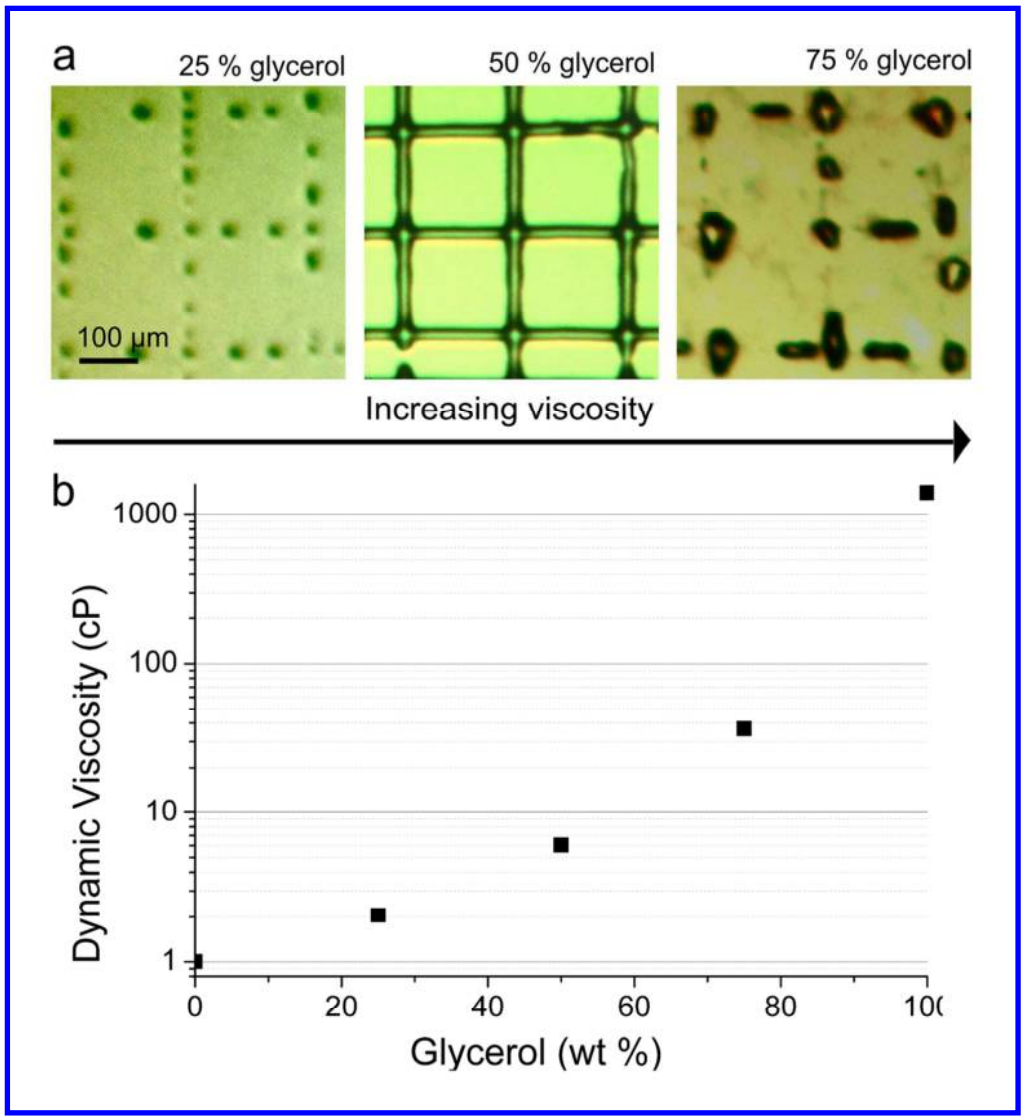
a
25 % glycerol
50 % glycerol
75 % glycerol
100 µm
Increasing viscosity
b
Dynamic Viscosity (cP)
1000
100
10
1
0
20
40
60
80
100
Glycerol (wt %)

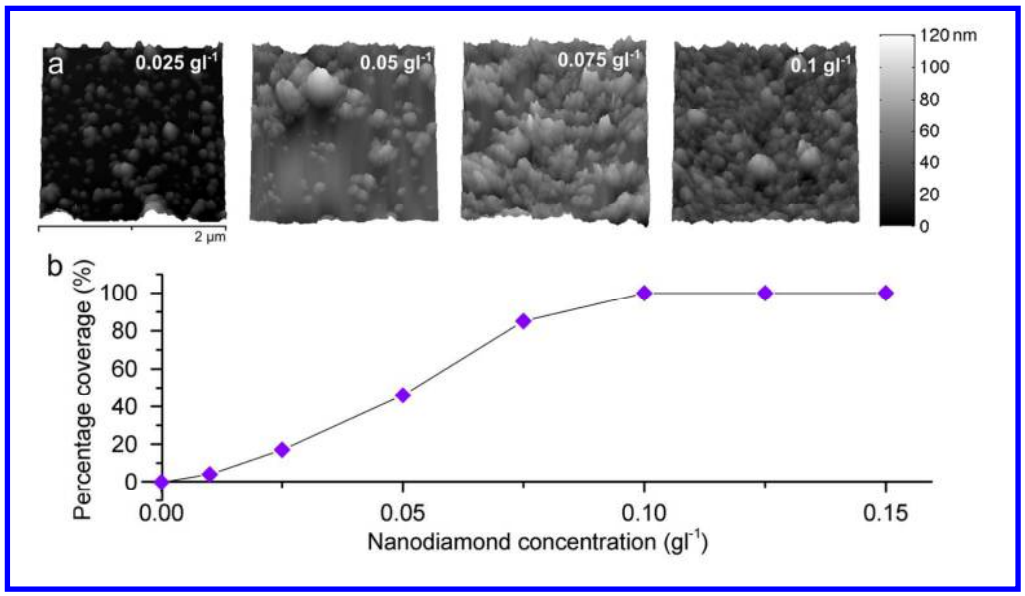
a
0.025 gl-1
0.05 gl-1
0.075 gl-1
0.1 gl-1
2 μm
120 nm
100
80
60
40
20
0
b
Percentage coverage (%)
100
80
60
40
20
0
0.00
0.05
0.10
0.15
Nanodiamond concentration (gl-1)

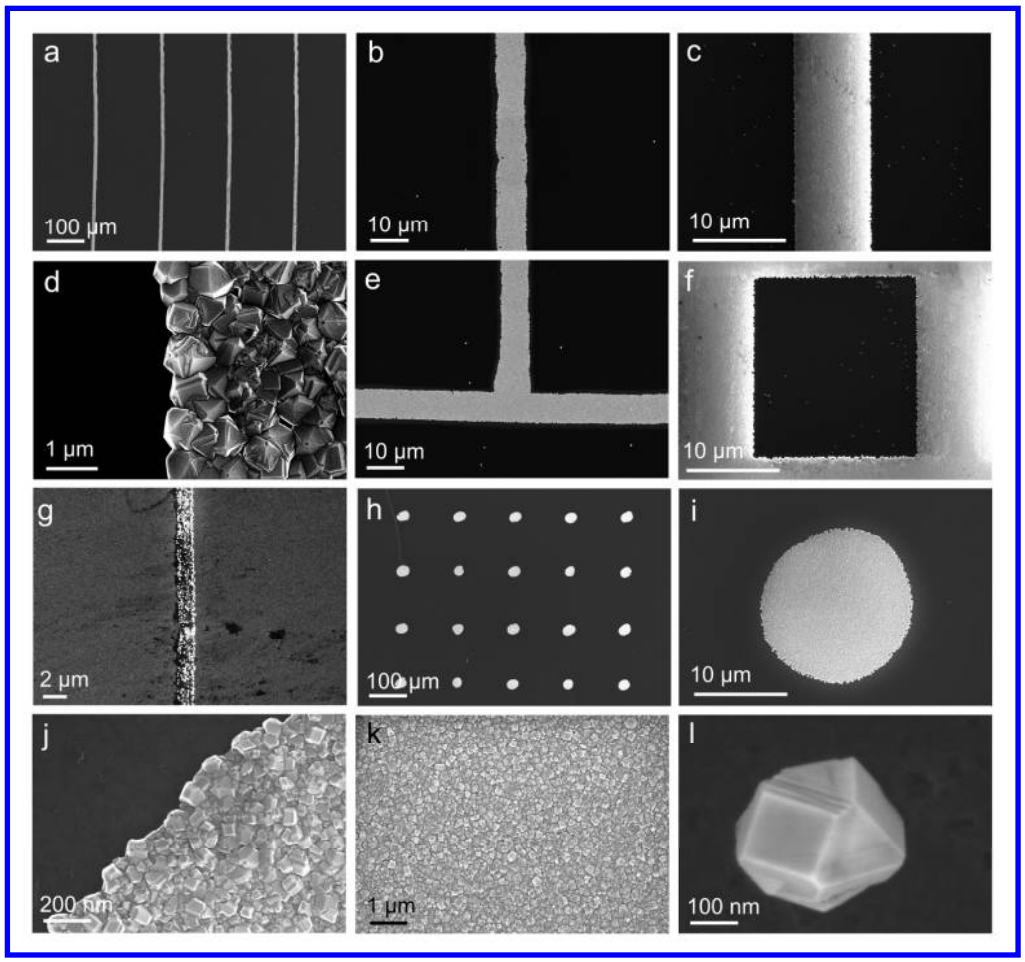

198x186mm (299 x 299 DPI)

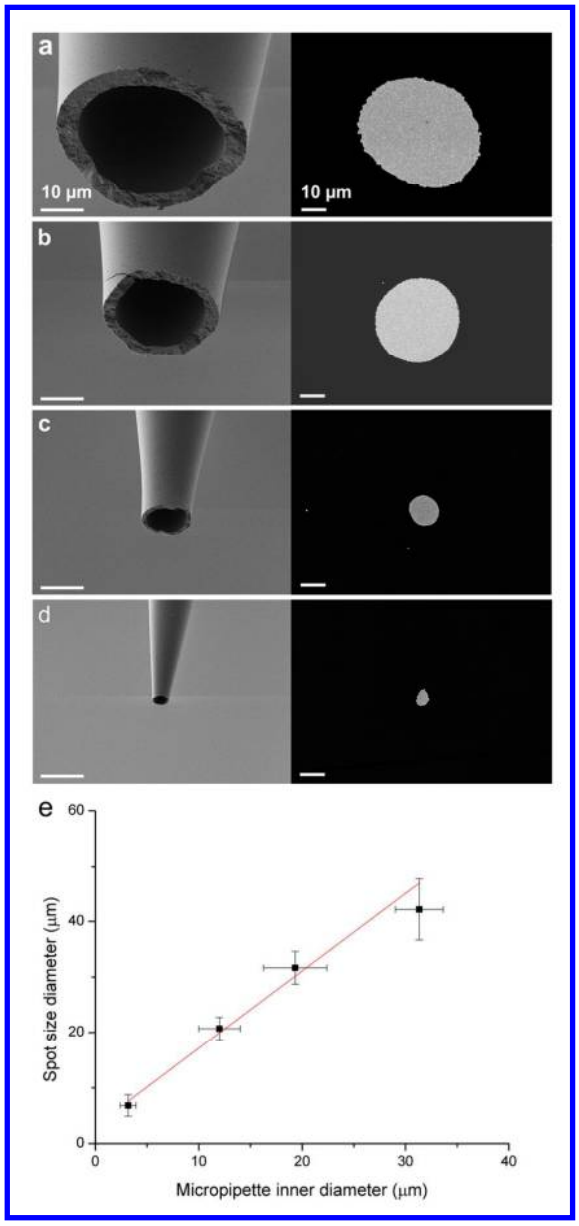
a
10 µm
10 µm
b
c
d
e
Spot size diameter (µm)
Micropipette inner diameter (µm)
0
20
40
60
0
10
20
30
40

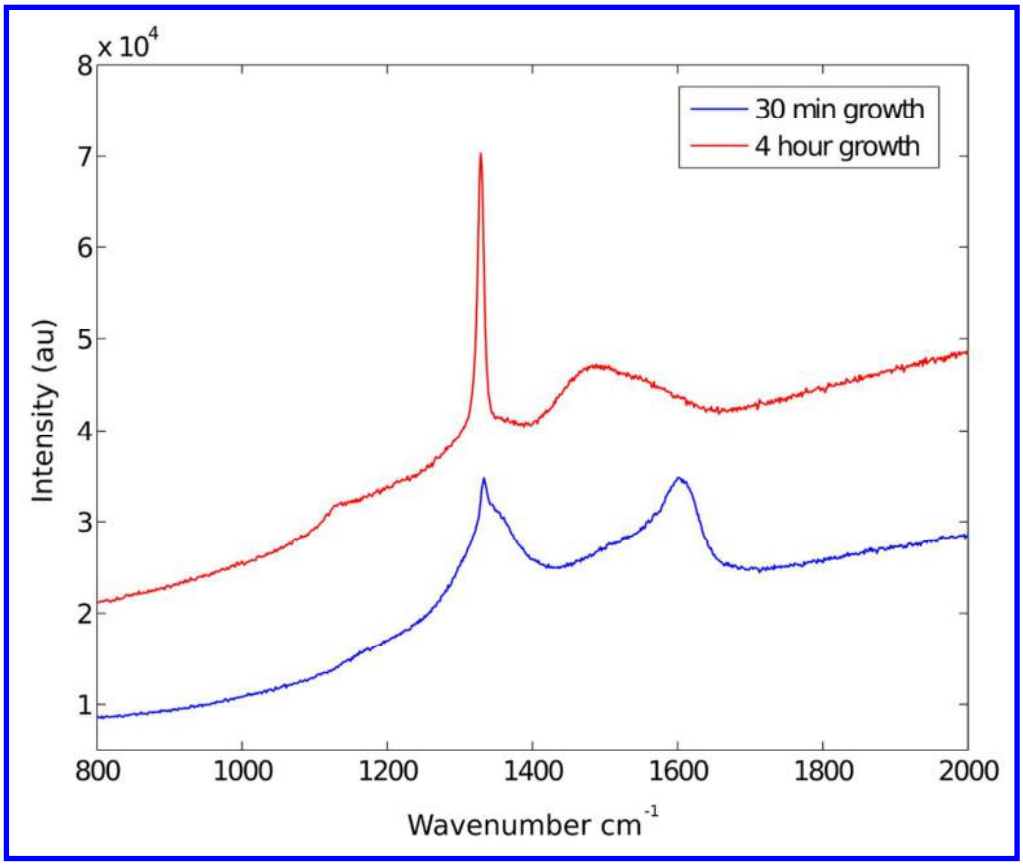
x 10^4
8
7
6
5
4
3
2
1
Intensity (au)
30 min growth
4 hour growth
800
1000
1200
1400
1600
1800
2000
Wavenumber cm^-1

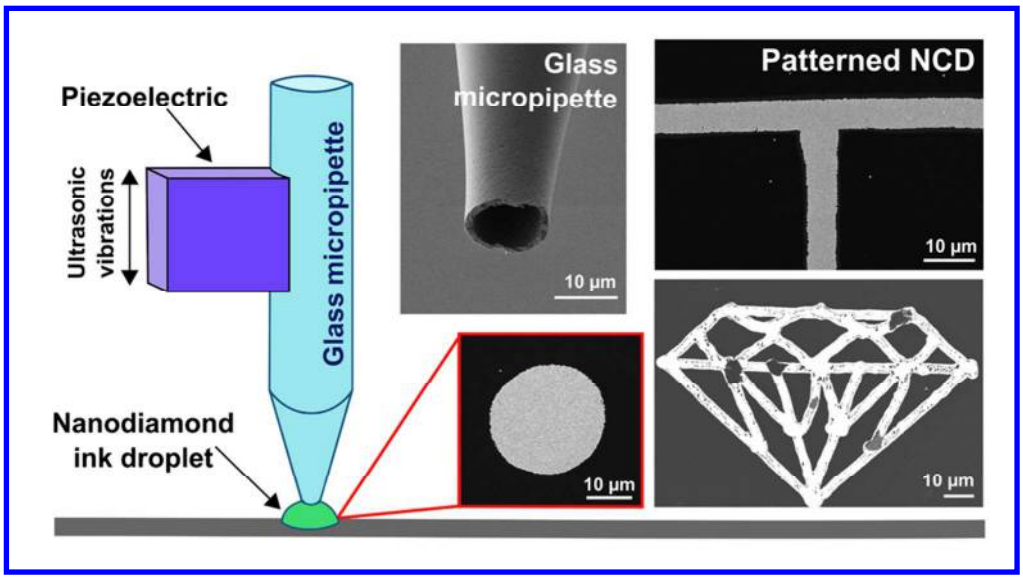

For table of contents only
85x47mm (300 x 300 DPI)